Cavity QED with high-Q whispering gallery modes

D. W. Vernooy, A. Furusawa, N. Ph. Georgiades, V. S. Ilchenko,* and H. J. Kimble
Norman Bridge Laboratory of Physics 12-33, California Institute of Technology, Pasadena, California 91125
(Received 18 December 1997)

We report measurements of cavity-QED effects for the radiative coupling of atoms in a dilute vapor to the external evanescent field of a whispering-gallery mode (WGM) in a fused silica microsphere. The high Q (5×10^7), small mode volume (10^{-8} cm^3), and unusual symmetry of the microcavity evanescent field enable velocity-selective interactions between fields with photon number of order unity in the WGM and $\bar{N}_T\sim1$ atoms in the surrounding vapor. [S1050-2947(98)50904-3]

PACS number(s): 42.50.Ct

Cavity QED has proven to be a fertile arena in which to study coherent interactions between single atoms and photons [1]. In the optical domain, the cavities employed to achieve strong coupling have been Fabry-Perot microresonators with finesse $\mathcal{F}\sim10^5$, as in the initial work of Ref. [2] and continuing to the recent demonstrations of real-time cavity QED with individual atoms [3,4]. By contrast, the whispering gallery modes (WGMs) of quartz microspheres [5] offer an alternative avenue to the regime of strong coupling with the potential to surpass Fabry-Perot cavities with respect to certain key parameters in cavity QED. For example, such resonators have the capability of achieving extremely long photon storage lifetimes while maintaining a strong dipole coupling to an atomic [6], ionic [7], or molecular [8] species via the small volume of a single mode, leading to the potential for ratios of coherent coupling to loss mechanisms in excess of 10^3 [6] . Indeed, quality factors $Q\approx8\times10^9$ have been reported for wavelengths 633 nm $\leqslant\lambda\leqslant$852 nm, corresponding to finesse $\mathcal{F}\sim2.2\times10^6$ [9,10], which is the highest value on record for an optical resonator.

Motivated by these prospects, in this Rapid Communication we report measurements of the interaction of atoms with the external evanescent field of a whispering gallery mode in a domain in which cavity-QED effects become important. More specifically, we study the modifications of cavity transmission due to the coupling of $\bar{N}_T\sim1$ cesium atoms in a thermal gas with a single resonant WGM at the level of a few photons in the mode. The possibility for sensitivity to $\bar{N}_T\sim1$ atoms in the microsphere's evanescent field in the face of Doppler broadening of roughly 100 times the natural linewidth is a consequence of the features of the microspheres used here, namely, small size (with radius $a<60$ μm and mode volume $V_m\sim10^{-8}$ cm^3) and narrow linewidth (with $Q_1=5\times10^5\leqslant Q\leqslant Q_2=5\times10^7$). Although it is clearly desirable to reduce the Doppler broadening by coupling to cold atoms [3,4], our current experiments are an exciting initial step towards realizing the potential of WGMs for long-lived coherent dynamics in cavity QED.

The actual setup is depicted in Fig. 1 and consists of a grating stabilized diode laser of a few hundred kHz linewidth coupled into a microsphere via frustrated total internal reflection from a prism [5]. The microspheres are fabricated from low-OH fused silica of index $n=1.452$ using an oxygen-hydrogen microtorch [11] and then mounted inside the vacuum system. The range $Q_1\rightarrow Q_2$ is accessed by using different spheres and various modes of the same sphere, by loading the bare Q of any individual mode with the prism outcoupler, and by waiting for the gradual degradation of the Q due to repeated contact of the sphere with the prism. In fact, it is necessary to couple to higher-order WGM radial modes ($p\sim3-4$) in order to maintain an acceptable coupling efficiency, as the incoupling optics are mounted outside the vacuum chamber. In addition, the light is injected off of the horizontal symmetry plane of the microsphere by an angle $\Theta\sim10°-15°$ to take advantage of the slight ellipticity of the spheres (typically $\sim$3%) and excite the so-called precessing modes [12,13], thus allowing the direct emission from a WGM to be separated from the reflected exciting beam and collected onto a photomultiplier. We emphasize that this technique provides a directly transmitted beam analogous to that from a partially transmitting output coupler in a ring cavity, with the details of the excitation protocol and mode identification discussed in more detail in Refs.

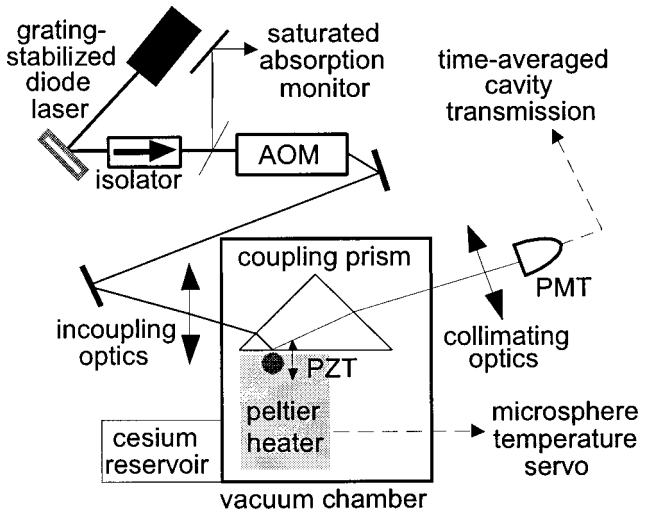

FIG. 1. A simplified schematic of the experimental setup is shown with detailed discussion in the text. The microsphere is indicated by the dark circle at the face of the coupling prism and is surrounded by a dilute atomic cesium vapor.

*Permanent address: Department of Physics, Moscow State University, Moscow 119899, Russia.

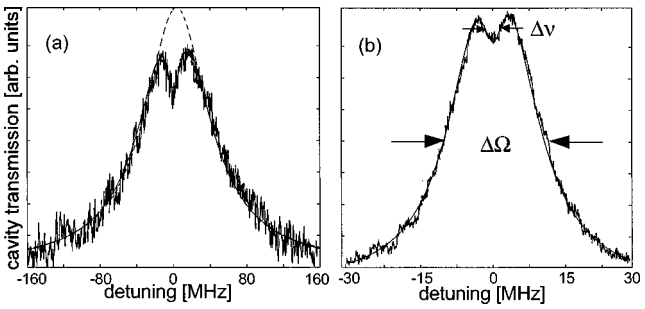

FIG. 2. The transmitted intensity $T(\omega_L)$ for single WGMs is shown for (a) $Q=1.5\times10^6$ and (b) $Q=4\times10^7$. In the regime of (a), we infer from a phenomenological model [solid line, see Eq. (3)] that the dip width is driven by a set of atoms selected by the cavity geometry. As the Q increases (b), the width of the absorptive feature narrows, suggestive of a class of atoms with small velocity. Zero detuning corresponds to the common atom-cavity resonance ($\omega_L=\omega_a=\omega_c$). The inferred empty cavity transmission is indicated in (a) (dashed line).

[12,13]. Estimates for the mode numbers (l,m) are given by $l\sim 2\pi na/\lambda$ for the orbital mode number and $m=l\cos\Theta$ for the azimuthal index, with both TE and TM polarizations included in our study. We thus isolate a single traveling-wave mode (p,l,m) that is degenerate *only* with the counterrotating $(p,l,-m)$ mode, which for $Q\lesssim 5\times10^7$ is unexcited, as evidenced by the absence of any resolved doublets in the transmitted intensity [14].

By thermally contacting the microsphere assembly to a Peltier element and monitoring temperature changes with a thermistor [15], a given cavity resonance ω_c is passively stabilized to the frequency ω_a of the $F=4\leftrightarrow F'=5$ hyperfine transition of the cesium $D2$ line (lifetime $\tau=1/2\gamma\simeq 32$ ns) at $\lambda_a=852$ nm, with residual thermal drifts of the cavity mode being $\sim\pm500$ kHz over 10 min. A piezo-controlled translation stage is mounted inside the vacuum chamber to give fine control of the prism-sphere distance. The vacuum system itself is pumped to a background pressure of 10^{-8} Torr and contains a thermal cesium reservoir, leading to an atomic density of typically 2×10^9 atoms/cm^3, as monitored by optical absorption in the vapor. Under the assumption that this background cesium density is a fair representation of the atomic density in the evanescent field, the total mode volume external to the sphere $V_m^e\sim5\times10^{-10}$ cm^3 implies that $\overline{N_T}\sim1$ atom interacts with the mode.

Our procedure for data acquisition is to scan the frequency of the incident laser while recording the intensity transmitted by the microsphere, with averaging times of several minutes required to achieve an acceptable signal-to-noise ratio. The frequency of the incident laser is independently monitored via saturated absorption spectroscopy in a separate cesium cell. For small frequency scans of ±25 MHz, a second method consists of FM locking of the laser to the atomic line and frequency scanning using a double-passed acousto-optic modulator. As shown in Fig. 2 for the case of coincident cavity ω_c and atomic ω_a resonance frequencies, sub-Doppler features are clearly observed as ''absorption dips'' in the transmission spectrum $T(\omega_L)$. Other scans demonstrate that when ω_c is tuned away from ω_a, the absorptive feature in $T(\omega_L)$ does not similarly shift.

From data such as those in Fig. 2 over a range $Q_1\leqslant Q\leqslant Q_2$, we plot in Fig. 3 the width $\Delta\nu$ of the narrow absorption feature versus the *inverse width* $\Delta\Omega^{-1}$ of the broad transmission function, with $(\Delta\nu,\Delta\Omega)$ defined in Fig. 2. Note that $\Delta\Omega$ serves as an indirect measure of the linewidth of the empty cavity and hence of Q^{-1} via $q\equiv\omega_c/\Delta\Omega$ [16]. Given that the Doppler half width at half maximum (HWHM) in the cesium vapor is $\Delta\omega_d\sqrt{\ln2}/2\pi\sim190$ MHz and that the data in Fig. 3 are taken in a linear regime, it is perhaps surprising that $\Delta\nu\ll\Delta\omega_D$. Operationally, we ensure that the data are acquired in a linear regime with measurements of the sort shown in Fig. 4(a). For a specific mode with $Q\sim1.5\times10^6$, the depth of the absorptive feature on resonance as a function of the transmitted intensity on resonance is seen to exhibit a linear relation up until $m_0\sim10$ intracavity photons, beyond which it begins to saturate. More generally, we estimate the intracavity photon number m_0 to vary between $0.5\leqslant m_0\leqslant30$ for our data, with saturation for $m_0\gtrsim10$.

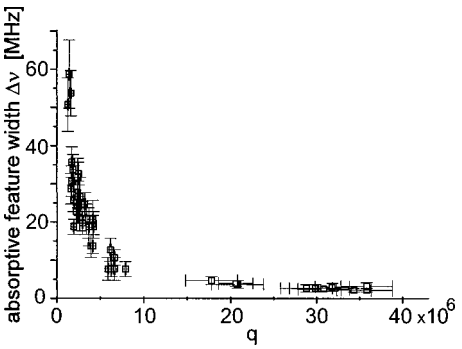

FIG. 3. The width $\Delta\nu$ of the absorptive feature plotted against $q\equiv\omega_c/\Delta\Omega$ ($\Delta\nu$, $\Delta\Omega$ defined in Fig. 2), where the relationship of q to the actual mode Q is discussed in the text.

Our starting point, in an attempt to model these observations, is the Heisenberg equations of motion for a set of moving atoms coupled to a single WGM in the weak-field limit [17]. The transmission function $t(\omega_L)$ for the ratio of transmitted to incident field amplitudes is derived assuming a time-independent steady state for the intracavity field and classical atomic trajectories unaffected by the cavity field, and is found to be

$$t(\omega_L)=\frac{\kappa}{\kappa-i\delta_c+g_0^2\overline{N_T}\chi(\omega_L)}, \tag{1}$$

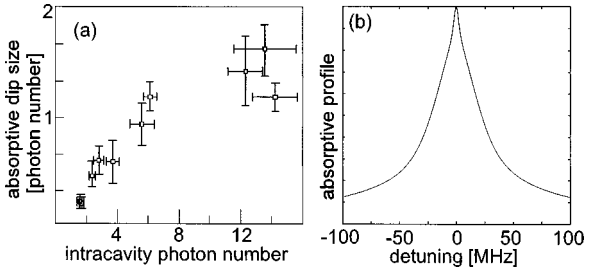

FIG. 4. (a) Dependence of the size of the narrow absorption dip on intracavity photon number in the low-Q regime of Fig. 2(a). (b) The atomic response $|\chi_A(\omega_L)|^2$ (normalized to unity) inferred from the phenomenological model discussed in the text [see Eq. (3)].

where $\kappa=\omega_c/2Q$ is the cavity HWHM with no atoms and $\delta_{c,a}=\omega_L-\omega_{c,a}$ are the cavity and atomic detunings. For a mode volume V_m and mode function $\psi(\mathbf{r})$, the atomic dipole coupling rate for a single atom is described by a vacuum Rabi frequency $g(\mathbf{r})=g_{\max}\psi(\mathbf{r})$ with $g_{\max}=\sqrt{3c\lambda^2\gamma_\perp/4\pi V_m}$, so that $g_0=g(a)$ is the value at the surface of the sphere (though the WGM field maximum is actually inside the sphere close to the surface, the maximum value accessible to the atomic vapor, $g_0/2\pi\sim 20$ MHz, is right at the surface). The quantity

$$\chi(\omega_L)\equiv\frac{1}{V_m}\int d^3\mathbf{v}p(\mathbf{v})\int d^3\mathbf{k}\frac{|\phi(\mathbf{k})|^2}{\gamma-i(\delta_a+\mathbf{k}\cdot\mathbf{v})} \qquad (2)$$

plays the role of an effective susceptibility for the atomic sample in its interaction with the WGM. The Fourier transform of the mode function

$$\phi(\mathbf{k})=(2\pi)^{-3/2}\int d^3\mathbf{r}\psi(\mathbf{r})\exp(-i\mathbf{k}\cdot\mathbf{r})$$

is normalized such that

$$V_m=\int d^3\mathbf{k}|\phi(\mathbf{k})|^2=\int d^3\mathbf{r}|\psi(\mathbf{r})|^2,$$

with the effective atom number $\bar{N}_T\equiv\rho V_m^e$ and ρ as the atomic density. $p(\mathbf{v})$ is the atomic velocity distribution, which is assumed to be Maxwell-Boltzmann.

Because we have been unable to evaluate $\chi(\omega_L)$ for the actual functions $\{\psi(\mathbf{r}),p(\mathbf{v})\}$, we have performed calculations for simplified approximations to $\psi(\mathbf{r})$ external to the microsphere (e.g., $\psi(\mathbf{r})\sim\exp[-2\pi(r-a)/\lambda]\exp(-\theta^2/\theta_0^2)\exp(\mathrm{im}\phi)$ as an approximation to $\psi(\mathbf{r})\sim h_l^{(1)}(kr)Y_{lm}(\theta,\phi)$). Via numerical integration, we find transmission functions $T(\omega_L)\equiv|t(\omega_L)|^2$ that are in quantitative accord with the measured spectra for low $Q\lesssim Q_0=5\times10^6$, but which deviate from our observations for $Q\gtrsim Q_0$ due to a near absence of *narrow features of width* $\sim\gamma$.

Nonetheless, these calculations motivate an ansatz that takes

$$\chi(\omega_L)\rightarrow\chi_A(\omega_L)\equiv\frac{1}{\bar{N}_T}\left(\bar{N}_d f_d(\delta_a)+\frac{\bar{N}_t}{\Delta\omega_t-i\delta_a}+\frac{\bar{N}_a}{\gamma-i\delta_a}\right), \qquad (3)$$

with $\bar{N}_d+\bar{N}_t+\bar{N}_a=\bar{N}_T$. The first component in Eq. (3) is physically motivated by noting that there must be a Doppler-broadened response $f_d(\delta_a)\sim(1/\Delta\omega_d)\exp(-\delta_a^2/\Delta\omega_d^2)$ due to velocity components tangential to the sphere in the direction of circulation of the mode. In addition, due to the geometry of the WGM, there is also significant transit broadening due to residence times of only $10^{-2}\tau$ for motion along the radial coordinate to $10^{-1}\tau$ along the $\hat{\mathbf{e}}_\theta$ direction (for which there is no Doppler broadening). Though any given atomic trajectory will yield a complicated function of both of these mechanisms [as in Eq. (2)], in Eq. (3) we simply *add* a transit broadened component of HWHM $\Delta\omega_t/2\pi\sim 25$ MHz corresponding to a linear trajectory of length $l_t\sim\sqrt{a\lambda/\pi}$ through the mode.

The solid lines through the data of Fig. 2 are based on Eq. (1) with the ansatz of Eq. (3). For $Q\lesssim Q_0$, only the first two components with $\bar{N}_d=0.75\pm0.05$ and $\bar{N}_t=0.25\pm0.03$ are needed in order to explain *all traces*. From this, we infer that the Doppler-broadened set of atoms act only as a broad absorber (since $\Delta\omega_t<\kappa<\Delta\omega_d$) and that the absorptive dip at line center is accounted for by the width $\Delta\omega_t$, implying that cavity geometry is a dominant factor below Q_0. That is, the geometry of the cavity correctly accounts for the coexistence of both transit and Doppler broadening, where of course the simple sum of contributions suggested phenomenologically in Eq. (3) is more properly interpreted as an interplay of frequency scales as in Eq. (2).

By contrast, for $Q>Q_0$ it is essential to include a small component $\bar{N}_a\sim0.015$ of atoms that respond with their natural linewidth γ (the inclusion of which does not change the quality of the fits for $Q\lesssim Q_0$). In fact, this component now completely determines the properties of the narrow absorptive feature, since $\kappa<(\Delta\omega_t,\Delta\omega_d)$. Although the need for this small subset of atoms moving slowly enough and in directions such that they are neither appreciably Doppler- nor transit-broadened is thus operationally motivated, their existence is also supported within the context of other measurements near dielectric surfaces, as, for example, in the work on Doppler-free evanescent-wave spectroscopy [18].

Our simple model also allows us to address the issue of the relationship of the quantity q of Fig. 3 to the actual empty cavity Q. For $Q\lesssim Q_0$ we have that $q\approx Q$, with our inference of the empty cavity transmission shown as the dashed trace in Fig. 2(a). However, for $Q>Q_0$, the two broadly absorbing components in $(\bar{N}_d,\bar{N}_t)$ (which account for most of the atoms) significantly alter the line shape relative to that inferred for the empty cavity with $q\simeq Q/2.5$ for $Q=Q_2$ and the peak transmission of the cavity reduced by a factor ~4.5. In fact, within the context of our ansatz for χ_A, the subnatural widths in Fig. 3 are an artifact of how these different contributions (each of width $\geqslant\gamma$) combine to produce $T(\omega_L)$, as shown by the solid curve in Fig. 2(b).

Finally, the results of our phenomenological model are summarized in Fig. 4(b), where we show the inference of the effective atomic susceptibility χ_A in Eq. (3) for $(\bar{N}_d,\bar{N}_t,\bar{N}_a)=(0.75,0.25,0.015)$, which best fits our data across the whole range in Q. Note that $\bar{N}_d+\bar{N}_t+\bar{N}_a\approx1$, which agrees rather nicely with our previous estimate based upon V_m^e and ρ. Interestingly, the profile of Fig. 4(b) bears a striking resemblance to those seen in ultrahigh-resolution molecular saturation spectroscopy in a transit broadening-limited regime [19].

Because $\bar{N}_a/\bar{N}_T\sim10^{-2}$, it is perhaps not surprising that our attempts to simplify the full integral of Eq. (2) failed to provide an accurate accounting of the narrow component of $\chi(\omega_L)$. Nonetheless, even assuming an exact evaluation, there are several mechanisms that could produce narrow features and are not accounted for in Eq. (1). First, as Q increases, a greater percentage of the counterpropagating $(q,l,-m)$ mode is excited, with a corresponding increase in the possibility for intracavity standing-wave structure [20] along the direction of mode propagation. Such structure is capable of producing narrow features by isolating the slow

atom components in a thermal gas. In addition, the $\exp(-\theta^2/\theta_0^2)$ dependence of our mode function in the transverse direction is strictly only valid for the $m=l$ mode with $\theta_0^2 \sim 2/l$, and, as one moves away from $m=l$, the WGM dependence on θ develops auxiliary maxima [21]. Second, $p(\mathbf{v})$ may depart from a Maxwell distribution, especially for those atoms with $v_r > 0$ that are leaving the surface. Obviously, a distribution that was peaked at lower velocities or that favored directions orthogonal to the direction of propagation of the mode would lead to narrow features. Finally, we have not accounted for possible atomic level shifts [22] ($\delta_a \rightarrow \delta_a + \Delta$) and modifications to the width ($\gamma \rightarrow \gamma'$) due to enhancement or inhibition [23,24] of radiative decay in the vicinity of the sphere's dielectric boundary, which would be extremely difficult to do correctly (e.g., by taking into account both nonidealities such as asphericity, which splits the degeneracy in mode number m and Q's that are typically nonradiatively limited, *and* the spatial dependence of γ' and Δ).

In conclusion, we have reported evidence for atoms interacting with high-Q WGMs at the level of a single atom and a few photons in the mode. An exact analysis of the interaction and hence direct comparison with theory is complicated by both geometrical effects of the sphere, precise details of the WGM mode structure, and the fact that most atoms transit the mode volume at their thermal velocity. However, the present effort opens the door for future experiments in which we hope to mitigate the fast transit effects and entirely change the velocity distribution by coupling cold atoms in a magneto-optical trap to the evanescent portion of the mode. A next goal would then be to watch *in real time* as individual atoms interact with the field in the spirit of Refs. [3,4]. In fact, it is extremely encouraging that the requirements of strong coupling, $\{g_0/2\pi \approx 20$ MHz$\} > \{(\kappa_{Q_2}, \gamma)/2\pi \approx (7$ MHz,2.6 MHz$)\}$, necessary for future work have already been achieved in this initial demonstration, but any manifestation (such as a resolved vacuum-Rabi splitting) has been masked by the atomic thermal distribution.

V.I. acknowledges fruitful discussions with J.-F. Roch. This work was supported by ONR Grant No. N00014-96-1-0580, the NSF, and DARPA via the QUIC Institute administered by ARO. D.W.V. acknowledges support from NSERC.

[1] H. J. Kimble, Philos. Trans. R. Soc. London, Ser. A **355**, 2327 (1997).
[2] G. Rempe *et al.*, Phys. Rev. Lett. **23**, 1727 (1991).
[3] H. Mabuchi, Q. A. Turchette, M. S. Chapman, and H. J. Kimble, Opt. Lett. **21**, 1393 (1996).
[4] C. J. Hood, M. S. Chapman, T. Lynn, and H. J. Kimble, Phys. Rev. Lett. (to be published).
[5] V. B. Braginsky, M. L. Gorodetsky, and V. S. Ilchenko, Phys. Lett. A **137**, 393 (1989).
[6] H. Mabuchi and H.J. Kimble, Opt. Lett. **19**, 749 (1994).
[7] V. Sandoghdar *et al.*, Phys. Rev. A **54**, R1777 (1996).
[8] D. J. Norris, M. Kuwata-Gonokami, and W. E. Moerner, Appl. Phys. Lett. **71**, 297 (1997).
[9] M. L. Gorodetsky, A. A. Savchenkov, and V. S. Ilchenko, Opt. Lett. **21**, 453 (1995).
[10] D. W. Vernooy *et al.*, Opt. Lett. **23**, 247 (1998).
[11] M. L. Gorodetsky and V. S. Ilchenko, Laser Phys. **2**, 1004 (1992).
[12] J. C. Swindal, D. H. Leach, and R. K. Chang, Opt. Lett. **18**, 191 (1993).
[13] M. L. Gorodetsky and V. S. Ilchenko, Opt. Commun. **113**, 133 (1994).
[14] D. S. Weiss *et al.*, Opt. Lett. **20**, 1835 (1995).
[15] V. S. Ilchenko and M. L. Gorodetsky, Laser Phys. **2**, 1004 (1992).
[16] Though clearly desirable, we have not recorded $T(\omega_L)$ in the absence of Cs atoms, since this would involve either tuning the sphere resonance $\gtrsim$500 MHz outside the Doppler line or pumping the atoms from the vicinity of the sphere, as with a cold finger. With the present seup, it is impossible to maintain the sphere/prism gap constant (and hence Q) during either of these procedures.
[17] H. J. Kimble, in *Cavity Quantum Electrodynamics*, edited by P. Berman (Academic Press, San Diego, 1994).
[18] P. Simoneau *et al.*, Opt. Commun. **59**, 103 (1986).
[19] S. N. Bagayev *et al.*, Appl. Phys. B: Photophys. Laser Chem. **48**, 31 (1989); Ch. Chardonnet *et al.*, *ibid.* **59**, 333 (1994); J. Ye, L.-S. Ma, and J. L. Hall, IEEE Trans Instrum. Meas. **46**, 178 (1997).
[20] J. C. Knight *et al.*, Opt. Lett. **20**, 1515 (1995).
[21] J. C. Knight *et al.*, Opt. Lett. **21**, 698 (1996).
[22] E. A Hinds and V. Sandoghdar, Phys. Rev. A **43**, 398 (1991).
[23] D. Kleppner, Phys. Rev. Lett. **47**, 233 (1981).
[24] A. J. Campillo, J. D. Eversole, and H. B. Lin, Phys. Rev. Lett. **67**, 437 (1991).